International Journal of Mine Water, vol. 5 (3), (1986) 29 - 46

Printed in Madrid, Spain

STUDIES IN THE PREDICTION OF WATER INFLOWS TO LONGWALL MINE WORKINGS

R.N. Singh*, S. Hibberd** and R.J. Fawcett*

*Department of Mining Engineering,
**Department of Theoretical Mechanics,
University of Nottingham, University Park,
Nottingham, NG7 2RD, United Kingdom.

ABSTRACT

The paper decribes results of mathematical investigations into the prediction of mine water inflows to longwall coal workings. Numerical calculations are reported on the basis of experimentally deduced hydraulic conductivities above longwall panels. The effect of longwall working on hydraulic conductivities is investigated by mathematical analyses of stress and failure. Numerical calculations of mine water inflows are reported on the basis of mathematically inferred hydraulic conductivities. Results are correlated with field data.

INTRODUCTION

Longwall mining is the dominant method of coal extraction in the United Kingdom. National Coal Board production statistics (1983a, 1983b) indicated that longwall working accounted for over 80% of total output and over 92% of deep-mined coal in the 1982/83 financial year. Inflows of water have frequently disturbed longwall operations as reported by Orchard (1969), Saul (1970), Watson (1979), Pugh (1980) and Garritty (1982). Occurrences have varied from nuisance flows at around $2x10^{-3}$ $m^3 s^{-1}$ to serious inrushes of $8x10^{-2}$ $m^3 s^{-1}$. A particularly substantial flooding was reported by the Guardian (1983a, 1983b) and Times (1983) at the Wistow mine in the Selby coalfield where a total of $8x10^4$ m^3 of water poured through a longwall face at a rate of $2x10^{-1}$ $m^3 s^{-1}$. Common sources of water have been identified by Singh and Atkins (1982) as water-bearing aquifer strata, abandoned or disused workings, cavities formed by the dissolution of rock, cavities formed by bed separation between strata and surface accummulutions such as seas, lakes and rivers. The majority of inflows referred to above were from aquifers, although Pugh (1980) found that

bed separation cavities also played a role. Routine chemical analyses of mine water have indicated that water reaching undersea workings originated in aquifer strata rather than the sea itself (Whittaker and Aston, 1982 and Watson, 1979). Problems associated with water occurrences in mining operations, which have been summarised by Fawcett, Hibberd and Singh (1983), can be severe.

It is well established that the removal of coal by longwall methods causes damage to strata in the vicinity of the extraction. In many cases this disturbance opens the routes by which water reaches the working. Devices adopted to prevent water occurrences due to strata damage have included the prescription of a minimum cover for undersea workings (National Coal Board, 1971), the adoption of short face lengths (Saul, 1970 and Watson, 1979) and the pre-mining drainage of water by boreholes (Pugh, 1980). The first two methods always result in the sterilisation of coal reserves (Orchard, 1969) which may be unnecessarily high if the water risk is over-estimated. Watson (1979) noted that the Coal Board requirements resulted in the undersea workings of North East England experiencing only 30% as much water for each tonne of coal mined as the adjacent inland workings. An under-estimate of the water risk can lead to serious inrushes of the type noted in the Wistow mine.

RESEARCH OUTLINE

Accurate predictions of the water inflow rates associated with different longwall mining circumstances are highly desirable for reasons of safety, health and economy. The research described in this paper was conducted to develop mathematical modelling techniques for predicting inflows to longwall coal faces and to identify gaps in current knowledge which limited the application of such techniques. A major objective was to describe the strata damage specific to longwall workings and to investigate its effect on inflow rates. The first stage of the research comprised the development of numerical mine water inflow calculations based on experimental and qualitative knowledge of hydraulic conductivities near longwall extractions. The results of these calculations were employed to identify areas where further research was required. The effect of longwall working on hydraulic conductivities was consequntly investigated by means of mathematical analyses of stress and failure. Analytic and numerical results were obtained. Further mine water calculations were undertaken on the basis of models which incorporated the mathematically inferred hydraulic conductivities. Solutions were correlated with available field data. Early results have been reported by Singh, Hibberd and Fawcett (1985) and Fawcett, Hibberd and Singh (1986) and a more comprehensive account has been given by Fawcett (1986). A summary of the earlier papers and a more detailed report of later work is given in this paper.

NUMERICAL CALCULATIONS OF MINE WATER INFLOWS

Singh, Hibberd and Fawcett (1985) and Fawcett (1986) have described a series of numerical investigations into water inflow to longwall panels based on existing experimental and qualitative knowledge of fracture conductivities induced in overlying strata. Calculations were developed from a basic longitudinal section model in which two wedge-shaped zones of increased hydraulic conductivity due to fracturing extended upwards from the face. Undamaged conductivities applied below the mined seam, in front of the face wedges and above their upper limit. A consolidated zone continued behind the face wedges. All water reaching the working was

taken to originate in a source aquifer overlying the undamaged layer above the fractured zone. Variations were investigated within the constraints of the basic model.

Non-dimensional quantities, related to true physical values by appropriate scaling factors, were employed to give the results of calculations more general application. The non-dimensional unit length was taken to be the vertical distance between seam and aquifer. The computed pattern of water movement to a longwall panel was much more complex than the purely vertical flow assumed in mine water inflow models reviewed by Fawcett, Hibberd and Singh (1983). Heterogeneity induced by mining damage was the major cause of the complexity but anisotropic effects were also important. The thickness of undamaged rock underlying the aquifer was found to be crucial in determining water inflow rates. Reductions in its thickness down to a critical value caused small but steady increases in total inflow rates while further reductions beyond the critical value led to sudden and substantial increases. This behaviour, illustrated graphically in Figure 1, was observed under a variety of circumstances and the critical thickness was seen to vary with the ratio of horizontal to vertical conductivity in the undamaged protective layer. Flow rates at protective thicknesses above the critical value depended almost entirely on the hydraulic conductivity of the protective layer while only unprotected flow rates were affected appreciably by variations in conductivities in the wedge shaped zones of fracture damage. Constriction at the tips of these zones substantially limited unprotected flow, making it important to know whether the wedge representation near the face was adequate.

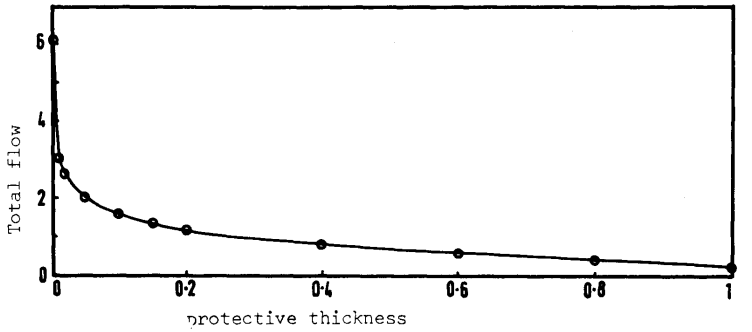

Figure 1 Total inflow rate v protective thickness for longitudinal section mine water inflow models

ANALYTIC CALCULATIONS OF HYDRAULIC CONDUCTIVITIES

Analytic calculations of hydraulic conductivities above a longwall face have been described by Fawcett, Hibberd and Singh (1986). The analytic model developed on the basis of stress determination, failure analysis and an assessment of the consequent fracture hydraulic conductivity. Stresses were calculated in two-dimensional cross section as the superposition of primitive values existing in the rock prior to

mining and the additional plane strain values induced by mining. The vertical component of primitive stress at any point was calculated from a formula for overburden weight while the horizontal component was obtained on the basis of a horizontal to vertical primitive stress ratio. Field results quoted by Brown and Hoek (1978) indicated that the primitive stress ratio could take any value below 4.0. Induced stresses were calculated from formulae involving the vertical component of primitive stress at seam level, the elastic constants of the rock mass surrounding the longwall working and the geometry of the excavation.

Total stresses were expressed as principal values from which failure could be determined. Modified compressive and tensile stresses were defined in terms of principal values to relate directly to unconfined rock strengths. Contour diagrams of their distributions were drawn to illustrate zones of compressive and tensile failure while straight lines indicated the orientations of tensile fractures and the major induced hydraulic conductivities. Models of a constant geometry were solved for primitive stress ratios between a plane strain value of 0.25 and a hydrostatic value of 1.0. Tensile and compressive failure heights were found to be similar in every case but the compressive zones extended further beyond the panel as illustrated in Figure 2. It was deduced that the fractures giving rise to increased hydraulic conductivities were initiated by compressive failure ahead of the face and beyond the gates and subsequently opened by tension over the panel. Tensile cracks were orientated downwards and towards the edges of the panel. Fracture heights depended heavily on the primitive stress ratio. Only the smaller values gave realistic results.

NUMERICAL CALCULATIONS OF HYDRAULIC CONDUCTIVITIES

Investigations of hydraulic conductivities were extended by means of finite element analyses. An iterative numerical approach was adopted in order to model post-failure characteristics and the partial roof support provided by closure. The solution procedure consisted of the three processes (a) assembly and solution of the stiffness matrix, (b) incorporation of closure, and (c) incorporation of rock failure repeated in the sequence (a), (b), (a), (c) until convergence was achieved.

Seam closure was incorporated by checking solution displacements at every opposing pair of nodes along the top and bottom surfaces of the mined region. If the convergence at any pair, given as the difference in vertical displacements, was greater than a maximum closure, specified as 0.9 times the extracted seam thickness, then both solution displacements were multiplied by a factor equal to the maximum closure divided by the solution convergence. Reduced displacements were incorporated as boundary conditions before repeating the stiffness matrix assembly and solution procedure. Predicted regions of closure were generally too small because local effects causing the complete disintegration and expansion of roof strata were not included. It was thought that such behaviour was unlikely to affect failure in strata more remote from the seam.

Rock failure was determined on the basis of stress calculations. Total stress components were used to calculate principal stresses and modified compressive stresses. Elements were tested row by row for compressive failure starting at the end furthest from the panel and working towards the centre line. Elements between the centre line and the first failed element identified in a row would have failed at an earlier

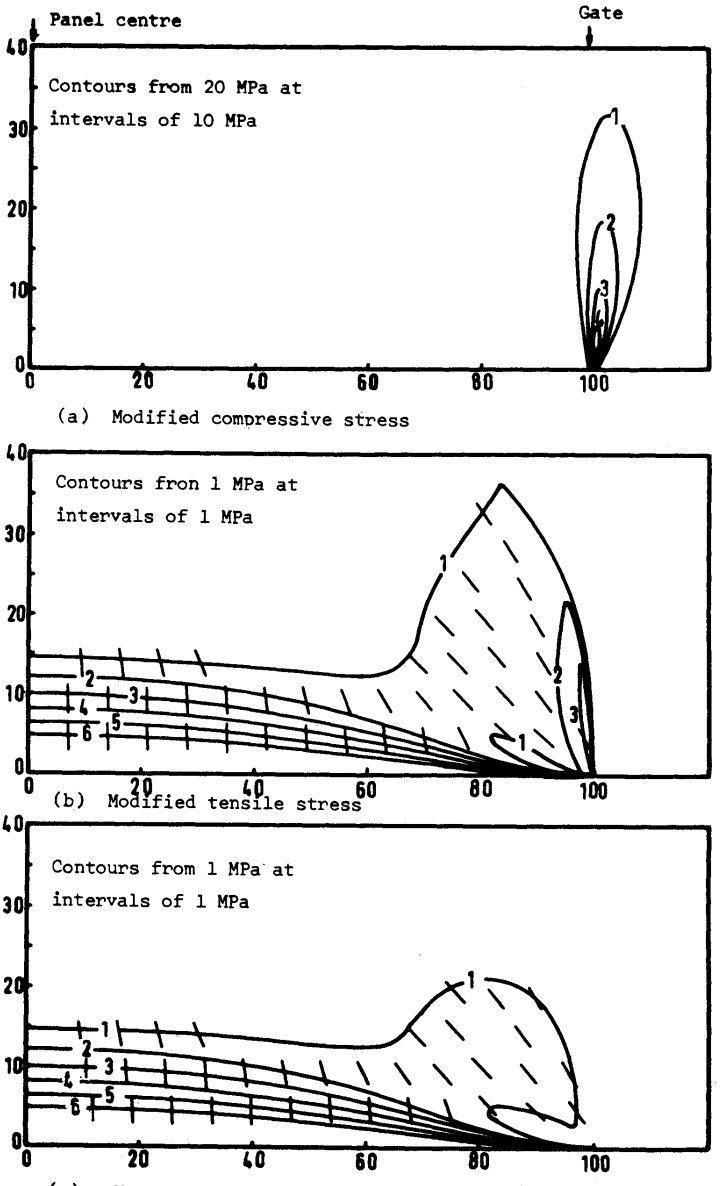

(a) Modified compressive stress

(b) Modified tensile stress

(c) Unmodified tensile stress

Figure 2 Contour diagrams of stress above a longwall panel with orientations of tensile failure

stage of the working and were treated accordingly. The test used for failure was whether the modified compressive stress exceeded the unconfined strength.

Boundary conditions consisted of zero normal displacements at remote boundaries and on the vertical line of symmetry through the panel centre, zero normal stresses at the ground surface and zero shear stresses at all non-mine boundaries. Induced stresses equal and opposite to primitive values were imposed at mine boundaries.

The validity of the computer code and the accuracy of the finite element solutions generated with it were tested by applying the program in non-iterative mode to an analytic model. Displacements were found to be highly accurate with a maximum error of 1.8% and the majority under 0.3%. Stress components were less accurate and errors of about 50% occurred near the vertical line through the gate singularity. They decreased to less than 9% at 25 metres above the gate and to less than 7% at 5 metres horizontal distance from it.

A set of models was devised to represent a range of panel widths, extraction thicknesses, principal stress ratios and seam depths. Pre- and post-failure elastic constants and unconfined compressive strengths were varied until approximate correlation was achieved with empirical results. Best-fit results were obtained when pre-failure elastic constants were assigned according to Table 1. The unconfined compressive strength was 15 MPa, post-failure conditions were represented by reductions in Young's moduli to one half of their original values and in the shear modulus to one quarter of its intact value and the primitive stress ratio was 0.25.

	Horizontal	Vertical
Young's moduli (Nm^{-2})	1.1×10^{10}	0.9×10^{10}
Poisson's ratios	0.19	0.17
Shear modulus (Nm^{-2})	0.5×10^{9}	

Table 1 Elastic constants used in the investigation

Results were obtained to assess the behaviour of fracture height as a function of depth, panel width and extraction thickness. Sixty three solutions are illustrated graphically in Figure 3 for depths of 800, 500 and 300 metres, panel half-widths of 100, 50 and 25 metres and extraction thicknesses from 0.9 metres to 2.7 metres at intervals of 0.3 metres. Four empirical formulae due to Chuen (1979) and Singh and Kendorski (1981) are reproduced for reference as broken lines. It can be seen that numerically predicted fracture heights were of the correct order in all circumstances and that the behaviour of fracture height as a function of extraction thickness was of the correct form for wide panels in deep seams. Under the latter circumstances, fracture height increased with extraction thickness until a maximum was reached when the support provided by closure was removed. Maximum damage above a panel of given width therefore occurred when the roof was supported entirely by pillars. Increases in extraction thickness in the absence of closure had no further

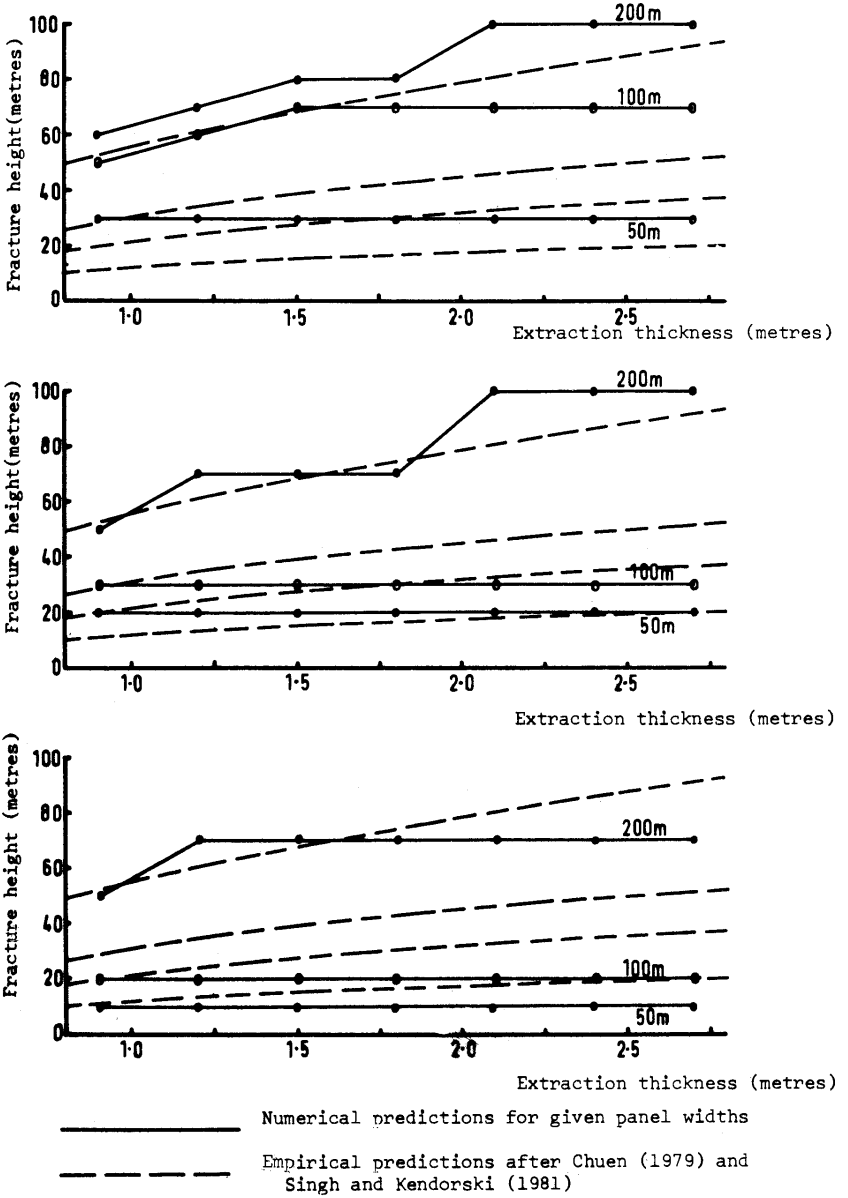

Figure 3 Fracture height as a function of extraction thickness at a primitive stress ratio of 0.25

effect on fracture height. Maximum fracture heights were reduced by narrower panel widths and shallower seam depths. Maxima imposed by the most narrow panels in the shallowest seams were so small that they were achieved at every extraction thickness. The extent of mining damage was smaller at shallow depths because primitive stresses and, in consequence, induced and total stresses were reduced.

The results also indicated that fracture heights above a longwall panel depended on the primitive stress ratio, elastic moduli and unconfined compressive strength of the surrounding rock mass. The primitive stress ratio was particularly important. Progressive increases from a plane strain value of 0.25 to a value of 2.0 led to drastic reductions in fracture heights. A further increase to 4.0 caused a substantial increase in failure under certain circumstances due to the combination of high horizontal compression and vertical stress relief. Such failure may correspond to bed separation. Smaller intact Young's and shear moduli led to reduced fracture heights consistent with different empirical predictive formulae quoted by Chuen (1979) for weak and strong roof strata. Reductions in the unconfined compressive strength were accompanied by larger fracture heights while smaller post-failure elastic moduli led to increased closure and occasionally to larger fracture heights.

An illustration of a typical hydraulic conductivity solution is presented in Figure 4. The diagram (a) represents the complete failure region divided into elements and labelled with the iteration numbers when failure was identified. Elements which remained intact contain no numbering. The mined seam lies along the horizontal line with zero vertical co-ordinate. The zero horizontal co-ordinate marks the panel centre while the gate is at a horizontal co-ordinate of 100. The diagram (b) identifies failed elements where at least one of the two principal stresses was tensile. Each straight line is perpendicular to the larger tensile stress and thus represents the orientation of the crack opened by tension in the failed element and the major direction of induced hydraulic conductivity. All failed elements identified by the diagram (a) would exhibit increased conductivity but values in elements emphasised in the diagram (b) would be especially large. The diagram (c) shows the distribution of modified compressive stress by means of contours. The second contour, corresponding to the simulated failure value of 15 MPa, retreated from the edges of the failed zone because of stress re-distribution after failure. The other contours indicate the approximate limits of the failed zone at different unmodified compressive strengths. The axes in all three diagrams are labelled in metres and refer to an origin at the centre of the floor of the longwall panel.

Graphical results indicated that the zone of failed rock surrounding a longwall extraction was bounded by a curve which reached two maxima extents above and below the seam and which retracted at the seam and at the upper and lower limits of failure. Field and laboratory results suggested that where this zone was still under substantial compression it would not possess an increased hydraulic conductivity. There was so little tendency for compression to diminish ahead of the face or beyond the gate that the zone of increased hydraulic conductivity could be regarded as limited to the regions directly above and below the panel.

A zone of omni-directional tension extended from the point of closure or panel centre to the coal edge and bounded by a horizontal line at a height of about 5 times the extraction thickness. The zone

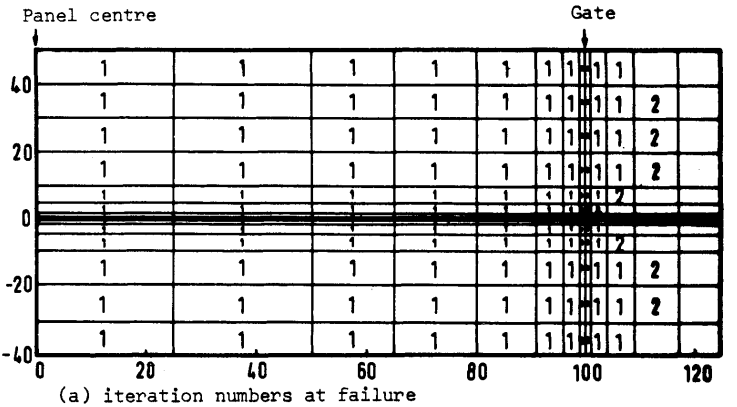

(a) iteration numbers at failure

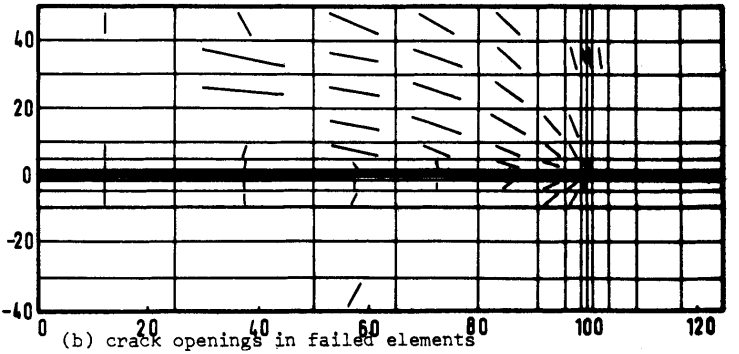

(b) crack openings in failed elements

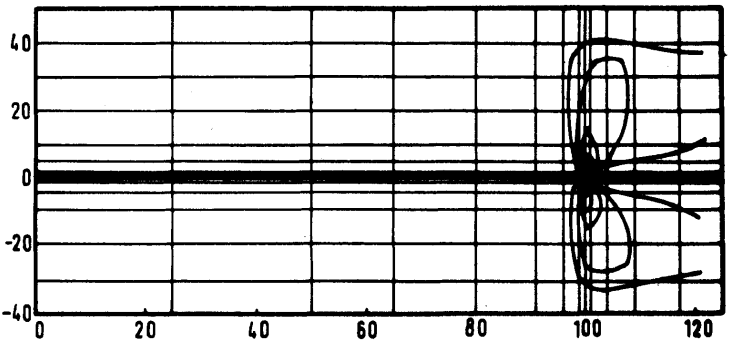

(c) contours of modified compressive stress increasing from 10 MPa at intervals of 5 MPa

Figure 4 Results of failure analysis due to longwall mining (extraction thickness 1.0m, panel half-width 100m, seam depth 300m)

coincided with the caved zone identified by Singh and Kendorski (1981) and Chuen (1979) and would be represented adequately in mine water inflow models as an extension of the mine sink.

Distributions of tensile stress suggested that hydraulic conductivities began to increase directly above or slightly ahead of the face and remained large over the whole of the open part of the seam. Major principal conductivities were directed downwards and outwards from the panel at between 30 and 60 to the horizontal. Their magnitudes reduced with vertical and horizontal distance from the gate and face while inclinations also decreased towards the panel centre. The tendency for strata to fail preferentially along bedding planes might cause the predicted steady reduction in conductivity angle to be replaced by a sudden change to the horizontal. Results suggested that the change occured about one sixth of the panel width from the gates and face.

If any portion of the seam became closed then the hydraulic conductivities above it were substantially reduced. Conductivities remained large above the whole of the open part of each seam, implying a representation of fractured zones close to the seam which was more rectangular than the experimentally deduced wedge configuration.

A MATHEMATICALLY DEDUCED MINE WATER INFLOW MODEL

Zones of fracture deduced by numerical calculation were represented for the purposes of mine water inflow modelling by the diagram illustrated in Figure 5. The calculations described by Singh, Hibberd and Fawcett (1985) demonstrated that water inflow to the floor of a longwall panel was negligible in comparison with inflow to its roof. Consequently the position of water withdrawal was represented by a simple line sink at the upper limit of the caved zone. Distances were assigned non-dimensional values and the most appropriate unit of length was taken as the vertical separation of mine sink and source aquifer. Region 1 represented undisturbed rock beyond the gate and an undamaged protective layer of thickness t above the fractured zone. Strata below the seam were also included in this region because increases in their conductivity were expected to have negligible effect on water inflow rates. Region 2, extending to 0.2 non-dimensional length units above the mine sink and 0.35 panel half-widths within the gate, represented failed strata subject to tensile stress or a substantial relaxation of compressive stress. The dominant conductivity within this region was inclined towards the gate at between 30^0 and 60^0 to the horizontal. Region 3, occupying the space between the top of region 2 and the upper limit of failure, represented failed strata subject to a smaller stress relaxation. Region 4 represented the remainder of failed strata over the open part of the mined seam. Hydraulic conductivities within this region remained large but their orientation changed so that the dominant direction lay along horizontal bed separation planes. The total length of the open part of the seam was set equal to 0.5 of the panel half-width. Region 5 represented failed strata undergoing compaction above the closed part of the extracted seam. Hydraulic conductivities were reduced relative to those in regions 2 to 4 but remained larger than the undisturbed values in region 1. The non-dimensional half-width of the panel was initially assigned a value of 5.0 for consistency with models reported by Singh, Hibberd and Fawcett (1985).

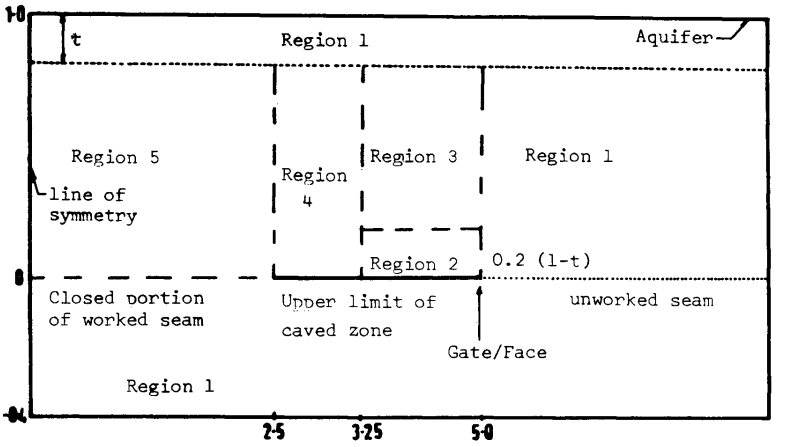

Figure 5 Geometry of mathematically deduced mine water inflow models

Hydraulic conductivities

Hydraulic conductivities were defined as multiples of the undisturbed horizontal value according to the list in Table 2. Major values in regions 1 to 5 were deduced on the bases of numerical investigations of hydraulic conductivity described in this paper and experimental results reported by Whittaker, Singh and Neate (1979). The vertical conductivity in region 1 was taken to be 0.01 of the corresponding horizontal value in common with models reported by Singh, Hibberd and Fawcett (1985). Fracturing within regions 2 to 5 led to anisotropic conductivities in which major and minor axes did not coincide with the horizontal and vertical directions. Minor conductivities in regions 2 to 5 were all set equal to one half of the residual major conductivity in region 5. Orientation angles defining the rotations from the horizontal co-ordinate axis to each major principal axis were assigned values of 30^0 in regions 2 and 3.

Region	Major principal conductivity	Minor principal conductivity	Orientation angle
1	1.0	0.01	0^0
2	60.0	5.0	-30^0
3	30.0	5.0	-30^0
4	40.0	5.0	0^0
5	10.0	5.0	0^0

Table 2 Hydraulic conductivities asigned to mine water inflow models

LONGITUDINAL SECTION CALCULATIONS

Solutions were obtained to a series of longitudinal section models for comparison with results reported by Singh, Hibberd and Fawcett (1985) and Fawcett (1986). The left hand boundary of Figure 5 was displaced in the negative horizontal co-ordinate direction to a position where it had negligible effect on flow. Solutions for protective thicknesses between 0.0 and 1.0 are listed in Table 3. Each flow range was defined as the distance between the two points on the aquifer where the rate of water discharge reached 10% of its peak value. Comparison with results from earlier wedge representation models revealed that differences in flow rates and ranges were substantial only at protective thicknesses less than 0.05. The flow rate for any model with a protective thickness greater than about 0.05 was determined chiefly by the hydraulic conductivity within the protective layer and was only slightly modified by differences in fracture conductivities. The flow rate for any model with a protective thickness less than 0.05 was dependent upon the precise nature of the fracture conductivities. There was a clear distinction between protected and unprotected flow regimes.

Protective thickness	Total flow	Range of flow	Centre of range
0.0	25.5	3.5	3.1
0.01	5.1	11.0	0.4
0.02	3.5	14.0	-1.0
0.05	2.1	22.2	-3.1
0.1	1.4	32.1	-5.1
0.15	1.1	39.2	-6.2
0.2	1.0	45.3	-7.2
0.4	0.6	61.8	-8.5
0.6	0.5	69.9	-7.7
0.8	0.3	71.0	-5.2
1.0	0.2	59.3	3.8

Table 3 Numerical results from longitudinal section models

CROSS SECTION CALCULATIONS

The flow ranges from longitudinal section models were substantial. It seemed unlikely that water would migrate to the face from a position far behind it when it could reach a gate by travelling a much smaller distance. This suggested that longitudinal section calculations did not represent physical circumstances accurately and that cross section calculations would be more appropriate. These differed from longitudinal section models in the imposition of a left hand boundary at a zero horizontal co-ordinate to represent the line of symmetry through the panel centre. Cross section models were investigated at protective thicknesses between 0.0 and 1.0. The results are illustrated graphically in Figure 6. The range of flow was re-defined as the distance from the line of symmetry to the point where the water flux from the aquifer fell to 10% of its peak value. Most gate flows were about 0.5 of the corresponding face quantities with a minimum ratio occurring at a protective thickness of 0.4. The smaller flow rates resulted from

reductions in the ranges to less than 0.5 of the face ranges. The model with no protective layer possessed highly local flow, directed into region 3 and 4 in a manner similar to the corresponding face section model, and the total flow was consequently unchanged. This model was the only one in which the water flux from the aquifer fell to less than 10% of its peak value at the centre line. Models with protective thicknesses of 0.01 and 0.02 exhibited less local behaviour and showed moderate reductions in flow rates relative to face quantities.

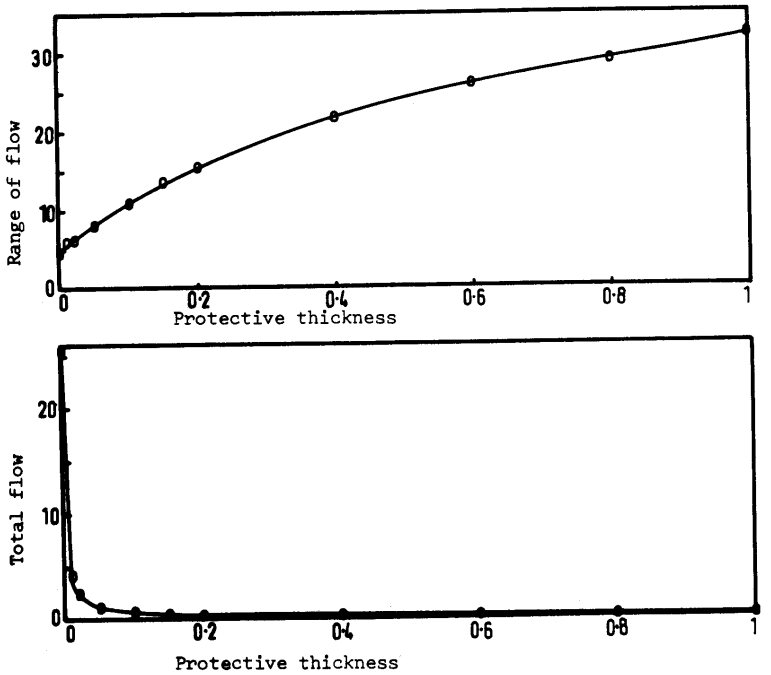

Figure 6 Range of flow and total inflow rates v protective thickness for cross-section mine water inflow models

Seepage velocities

Distributions of seepage velocities in the sequence of gate section models are illustrated in Figure 7. Comparison with earlier results of Singh, Hibberd and Fawcett (1985) and Fawcett (1986) revealed substantial differences from flows in wedge representation models at all protective thicknesses. The inclined nature of the fracture conductivities in regions 2 and 3 of the new models caused flow to be diverted towards the gate in every case. This contrasted with the earlier phenomenon whereby vertical flow through the wedges dispersed away from the face over the interior of the panel. Removal of the wedge tip constriction led to large increases in seepage velocities in the absence

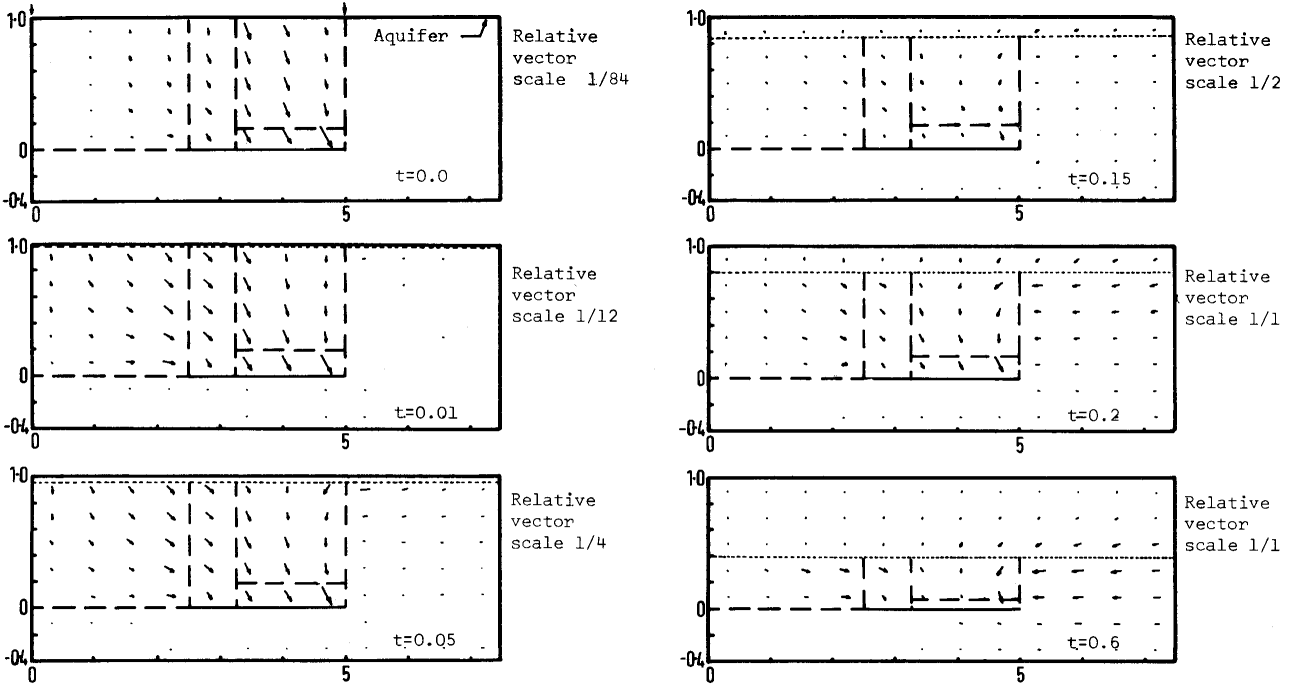

Figure 7 Distributions of seepage velocity in cross-section mine water inflow models at protective thicknesses t = 0.0, 0.01, 0.05, 0.15, 0.2 and 0.6

of a protective layer. At protective thicknesses between 0.02 and 0.6 water from parts of the aquifer beyond the gate entered the top of region 3 in a direction opposed to the major fracture conductivity. This phenomenon illustrated that directions of flow were determined partly by local anisotropy and partly by global heterogeneity.

Narrow panels

Water inflows were also calculated for a narrow panel. The new models were based on the geometry of Figure 5 with horizontal co-ordinates reduced by a factor of 5.0 to yield a panel half-width of 1.0 non-dimensional units. Flow rates were reduced at all protective thicknesses. The reduction in flow at zero protective thickness was proportional to the reduction in panel half-width while reductions at all other thicknesses were less severe. The ranges of flow were substantially diminished at small protective thicknesses but only slightly affected at larger values.

Steeply inclined fractures

A set of calculations was undertaken to determine the effect on water inflows of more steeply inclined fracture conductivities. The geometry of the narrow panel models was combined with the hydraulic conductivities of Table 2 except that the orientation angles in regions 2 and 3 were taken as -60^0. The change in orientation angle affected the total flow rate only at a zero protective thickness with a factor of increase equal to 1.7.

CORRELATION WITH FIELD RESULTS

The mine water inflow results described above were compared with measurements of physical water inflows documented by Aston (1982). The three inflows, to the E04, E51 and 1W panels in the High Main seam of the Horden Colliery, were identified as originating in a sandstone aquifer. The extracted seam was 2.5 metres thick and separated from the sandstone aquifer by 55 metres of mudstone and siltstone. A typical panel perimeter was 1500 metres with an average flow rate per metre of 3x10 m s . A limestone stratum formed a hydraulic connection between the sea bed and the sandstone aquifer so the difference between hydraulic heads at the source aquifer and the extracted seam was equal to the depth of the High Main seam below sea level. This depth was given by Saul (1970) in the range 250 to 300 metres. The caved height was deduced using a formula of Singh and Kendorski (1981) to lie in the range 7.5 to 15.0 metres. The distance corresponding to one non-dimensional unit was in the range 40.0 to 47.5 metres. Panel half-widths matched the narrow models most closely.

The measured figures were compared with numerical predictions to determine whether the inflows were protected or unprotected. Flows in the presence of a protective layer would depend upon the undamaged hydraulic conductivities of the mudstone and siltstone. The undisturbed horizontal conductivity was therefore taken as $1x10^{-11}$ ms^{-1} which implied a non-dimensional flow rate of $1x10^{4}$. Reference to Figure 6 showed that none of the models approached such a flow and it was therefore clear that the assumption of an intact layer above the fractured zone was inappropriate.

The non-dimensional flow rate to a narrow panel with no intact layer above the fractured zone fell in the range 5 to 10. The higher value implied a base conductivity of $1x10^{-8}$ ms^{-1} and a fracture conductivity in region 3 of $3x10^{-7}$ ms^{-1}. This was of the same order as values measured by Whittaker, Singh and Neate (1979), thus confirming that an unprotected model correctly described flow to the E04, E51 and 1W panels. A further confirmation was provided in a statistical analysis by Garritty (1983) which showed that the proportion of faces experiencing water inflows in excess of $2.0x10^{-2}$ $m^3 s^{-1}$ increased from 15% to 100% as the amount of cover to the Permian limestone decreased from 100 metres to 80 metres. The sudden increase would occur as fracturing reached the aquifer. The cover above the faces analysed in this section was only 55 metres so fracturing was certain to reach the aquifer.

CONCLUSIONS

The authors have successfully developed mathematical models of groundwater inflow to longwall coal panels and of hydraulic conductivities induced by longwall mining. Typical results have been reported. Mine water models have incorporated experimentally determined hydraulic conductivities and mathematically deduced values. Fracture height predictions have been correlated with empirical results and inflow predictions have been matched with field measurements. Parameters which are importent in determining induced hydraulic conductivities and mine water inflow rates have been identified.

It is proposed that the modelling of hydraulic conductivities and mine water inflows should be extended to include multi-panel workings, inclined strata and three-dimensional representations. These modifications will enable physical circumstances to be simulated more realistically. Time dependent effects will also be included in inflow modelling so that the loss of hydraulic head in the source aquifer as a result of water withdrawal can be represented. Further field work in the areas of primitive stress ratios and mining induced hydraulic conductivities would enable the validity of theoretical results to be tested more fully.

ACKNOWLEDGEMENTS

The authors wish to thank Professor T. Atkinson for his encouragement and the Science and Engineering Research Council for its financial support.

REFERENCES

Aston T.R.C, 1982, Hydrogeological aspects of rock mechanics and mining subsidence around longwall extractions, PhD thesis, Univ. of Nottm.

Brown E.T. and Hoek E., 1978, Trends in relationships between measured in-situ stresses and depth, Int. J. Rock Mech. Min. Sci., vol. 15, pp. 211-215

Chuen L.T., 1979, Practice and knowledge of coal mining under water bodies, Proc 10th World Mining Congress, Istanbul, vol 3., pp. III-15 1-15

Fawcett R.J., Hibberd S. and Singh R.N., 1984, An appraisal of mathematical models to predict water inflows into underground coal workings, Int. J. Mine Water, vol. 3, no. 2, pp. 33-54

Fawcett R.J, Hibberd S. and Singh R.N., 1986 Analytic calculations of hydraulic conductivities above longwall coal faces, Int. J. Mine Water, vol. 5, no. 1, pp.45-60

Fawcett R.J., 1986, Studies on the prediction of groundwater inflow to longwall coal faces, PhD thesis, Univ. of Nottm.

Garritty P., 1983, Water flow into undersea mine workings, Int. J. Mining Eng., vol. 1, no. 3, pp. 237-251

Guardian, 1983a, New mining techniques blamed for pit flooding, Tuesday July 26

Guardian, 1983b, NCB has to think again after the flood, Monday October 17
National Coal Board, 1971, Working under the sea, NCB Mining Dept., Instruction PI/1968/8 (Revised)

National Coal Board, 1983a, Report and Accounts 1982/3, NCB Purchasing and Contracts Office, London

National Coal Board, 1983b, Mechanisation profile number 25, NCB Statistics Dept.

Orchard, 1969, The control of ground movements in undersea working, Mining Engineer, vol. 128, part 5, pp. 259-273

Pugh W.L., 1980, Water problems at West Cannock no. 5 colliery, Mining Engineer, vol. 139, no. 221, pp. 669-679

Saul H., 1970, Current mine drainage problems, Mining Engineer, vol. 129, part 11, pp. 643-657

Singh M.M. and Kendorski F.S., 1981, Strata disturbance predictions for mining beneath surface water and waste impoundments, Proc. 1st Ann. Conf. Ground Control in Mining, Univ. of West Virginia, pp. 76-89

Singh R.N. and Atkins A.S., 1982, Design considerations for mine workings under accumulations of water, Int. J. Mine Water, vol.1, no. 4, pp. 35-56

Singh R.N., Hibberd S. and Fawcett R.J., 1985, Numerical calculation of groundwater inflow to longwall coal faces, Proc. 2nd Int. Mine Water Congress, IMWA, Granada, vol. 1, pp. 541-552

Times, 1983, Pitting their wits against water, Wednesday August 24

Watson H.F., 1979, Undersea coal mining in north east England, Proc. 10th World Mining Congress, Istanbul, vol. 3, pp. III-3 1-20

Whittaker B.N. and Aston T.R.C, 1982, Subsidence effects in the undersea coalfield workings of North East England, Proc. 1st Int. Mine Water Congress, IMWA, Budapest, vol. A, pp. 399-419

Whittaker B.N, Singh R.N. and Neate C.J., 1979, Effect of longwall mining on ground permeability and subsurface drainage, Proc. 1st Int. Mine Drainage Symp., Denver, Colorado